A new proposal prototype dedicated to validate unknown parameter identification method of heating source

Sara Fakih, Mohamed Salim Bidou, Thanh Phong Tran, L. Perez, Laurent Autrique

Experimental prototype to validate a method for solving an inverse heat conduction problem

Sara FAKIH[1], Mohamed Salim BIDOU[1], Thanh Phong TRAN[1], Laetitia PEREZ[1][0000−0001−6340−0317], and Laurent AUTRIQUE[1][0000−0002−7611−4923]

LARIS, Polytech, University of Angers, 49000 Angers, France
{sara.fakih,mohamedsalim.bidou,thanhphong.tran,laetitia.perez,laurent.autrique}@univ-angers.fr

Abstract. This paper focuses on developing a prototype for identifying specific unknown parameters in real experimentation. The initial objective involves validating a mathematical model representing a 2D thermal system and governed by parabolic partial differential equations. This is achieved by refining the error between temperature measurements from an infrared camera in a real experimental setup, and the mathematical model outputs. The final objective of this research is the parametric identification of a stationary heat source using an iterative regularization method (the conjugate gradient minimization algorithm). The latter is chosen for its effectiveness in addressing challenges inherent in the inverse heat conduction problems, well-known as ill-posed in the Hadamard sense.

Keywords: conjugate gradient method · experimental prototype · inverse problems · parametric identification · thermal process.

1 Introduction

Mathematical models formulated through partial differential equations (PDEs) are widely employed in industrial and thermal engineering sciences to accurately describe experimental processes behavior and ensure precise parametric identifications for complex systems as obtained in [1–5]. In this context, solving inverse heat conduction problems (IHCPs) emerges as a crucial objective when certain parameters are unknown, often due to the limitations in measurement capabilities or the complexity of the system under investigation, [6–9]. However, it is well known that such IHCPs are ill-posed, as low measurement noises can highly affect the identification quality [10]. To address this, the conjugate gradient regularization method has been developed [11–13], which guarantees convergence toward an admissible value of the unknown parameter by minimizing the error between the observed and predicted data.

This approach has gained significant attention in numerous research papers dedicated to identifying and controlling unknown parameters in a finite time and across multidimensional domains. For instance, [14–20] explored control and identification of heat fluxes and trajectories in the context of 1D systems. In 2D

geometries, offline methodologies also involved finding the flux and trajectory, detecting failure time for heat sources, and identifying the control for finite time temperature stabilization [8, 21–28]. Whereas quasi-online approaches have integrated real-time data over sliding intervals for the adaptive selection of sensors for unknown mobile heat flux estimation, the identification of thermal conductivity, control, heat flux and trajectory, and failure times [15, 29–33], providing more precise and up-to-date information into the system dynamics. Similar strategies have been employed in 3D domains [34–36].

This paper primarily aims to validate a mathematical model of an experimental prototype, which then paves the way for identifying the heat flux of a fixed disk located on the lower face of an aluminum plate, using temperature data captured by infrared camera sensors and in the presence of measurement noise. The heat flux identification is solved using the conjugate gradient method by addressing its well-posed direct, adjoint, and sensitivity problems [13]. The paper is organized as follows: section 2 outlines the studied experimental process, its mathematical model and the inverse method for estimating the unknown parameter, while section 3 delves into the temperature data acquisition method and the numerical results of simulated temperature compared to real collected data. Finally, conclusions and future perspectives are proposed in section 4.

2 Physical system and mathematical model

2.1 Prototype description

The goal is to develop an experimental device in order to validate methods dedicated to parametric identifications (see for example [37]). This prototype matches with a proposed mathematical thermal model in a 3D space, which is equivalent to 2D under the condition of negligible heat transfers along the plate thickness, thus reducing computational time [37, 38]. A thin metal plate with high thermal conductivity is considered. To accommodate the budget in reality, the proposed material is aluminum (copper, silver, and gold cannot be used). Accordingly, an aluminum plate of reasonable thickness and size is placed on a heat-insulating support (Fig.1a).

The heat source used is an RS Pro plate consisting of coiled resistance wire and protected by a sturdy steel (Fig.1b). When conventional heating elements are too wide, this thin plate is employed in fitting into narrow spaces. It is supplied with insulated connectors and earth conductors for quick and safe installation, and the wires are reinforced where they meet the plate to increase durability and resistance to pressure. The heat source dimension is $70 \times 75\ mm$, the supply voltage is 230 $Va.c$ with a rated output of 220 W, and can provide a maximum temperature of $260°C$.

The Optris PI 640i is a small infrared thermal camera (Fig.1c). With housing size of only $46 \times 56 \times 90\ mm$ and a weight of 320 g (lens included), it is among the market's most compact thermal cameras, available from 6, 800€ (excl. VAT), software and I/O interface are included. With an optical resolution of 640×480

pixels, it provides very sharp real-time thermal images. It is connected with the comprehensive Optris PIX Connect analysis software, and can work over temperature range of $-20°C$ to $900°C$ (optional up to $1500°C$), with the spectral range of 8 to 14 μm. Its refresh rate is up to 125 Hz.

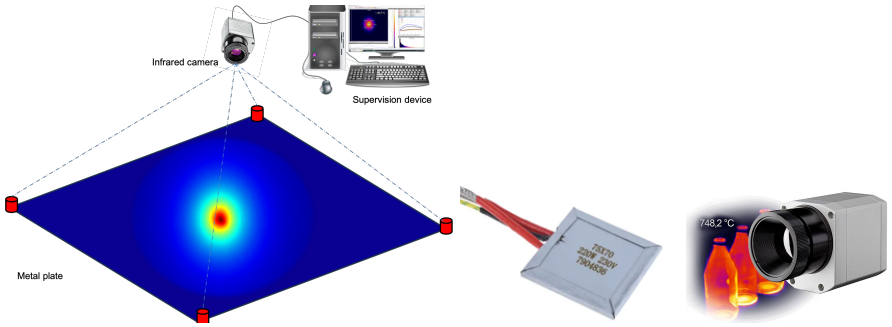

(a) Prototype description (b) Heat source (c) Infrared camera

Fig. 1. The experimental prototype main devices.

2.2 Mathematical model

In order to validate and model the experimental prototype, an aluminum plate $\Omega = \left]-\frac{L}{2},+\frac{L}{2}\right[\times \left]-\frac{L}{2},+\frac{L}{2}\right[\times \left]-\frac{e}{2},+\frac{e}{2}\right[\subset \mathbb{R}^3$ is considered, with lateral dimension L, thickness e, and boundary $\Gamma = \partial\Omega \subset \mathbb{R}^2$. The space variables (each measured in m) are $(x, y, z) \in \Omega$, and the time variable (in s) is $t \in T = [0, t_f]$, where t_f is the final time. The surface of Ω is heated by a thermal flux density $\phi(t)$ (in Wm^{-2}) acting on a homogeneous fixed disk D of center $I\left(x_s(t), y_s(t), z_s(t)\right)$ and radius r. Therefore, the plate temperature denoted by $\theta(x, y, z, t)$ (in °C), varies continuously $\forall(x, y, z, t) \in \Omega \times T$, [38]. Heat source total density function is defined by:

$$\Phi\left(x, y, z, t\right) = \begin{cases} \phi(t) & \text{if } (x, y, z) \in D\left(I(t), r\right) \\ 0 & \text{otherwise} \end{cases}$$

and could be expressed continuously and differentiably as in Eq.1 (see Table 1), where the regularized parameter $\eta \in \mathbb{R}^+$ is related to the heat flux discontinuity at the disk boundary. Without loss of generality, the time interval $T = [0, t_f] = \bigcup_{i=0}^{N_t-1} [t_i, t_{i+1}]$ is divided into N_t segments, with $t_i = \tau i$ and $\tau = t_f/N_t$. Thus, the density function is discretized as $\phi(t) = \sum_{i=0}^{N_t-1} \phi^i s^i(t)$, where $\phi^i = \phi(t_i)$, and the basis of hat functions for time discretization is $\forall i = 0, \ldots, N_t - 1$:

$$s^i(t) = \begin{cases} 1 + t/\tau - i & \text{if } t \in [t_{i-1}, t_i] \\ 1 - t/\tau + i & \text{if } t \in [t_i, t_{i+1}] \\ 0 & \text{otherwise} \end{cases}$$

Table 1. Literature of equations for unknown parameter identification based on the conjugate gradient method

No.	Description	Formula	Reference
Eq.1	**Total heat flux**	$\Phi(x,y,z,t)=\frac{\phi(t)}{\pi}\mathrm{arccot}\Big(\eta\sqrt{(x-x_s(t))^2+(y-y_s(t))^2+(z-z_s(t))^2}-r\Big)$	[35, 36]
Eq.2	**Laplace operator**	$\Delta\theta(x,y,z,t)=\frac{\partial^2\theta(x,y,z,t)}{\partial x^2}+\frac{\partial^2\theta(x,y,z,t)}{\partial y^2}+\frac{\partial^2\theta(x,y,z,t)}{\partial z^2}$	[35, 36]
Eq.3	**Direct problem**	$\begin{cases}\rho C\frac{\partial\theta(x,y,t)}{\partial t}-\lambda\Delta\theta(x,y,t)=\frac{\Phi(x,y,t)-2h(\theta(x,y,t)-\theta_0)}{e} & \text{on } \Omega\times T\\ \theta(x,y,0)=\theta_0(x,y) & \text{on } \Omega\\ -\lambda\frac{\partial\theta(x,y,t)}{\partial\vec{n}}=0 & \text{on } \Gamma\times T\end{cases}$	[30–33, 37–39]
Eq.4	**Cost function**	$J(\theta;\Phi)=\frac{1}{2}\int_T\sum_{n=1}^{N_c}\big(\theta(C_n,t;\Phi)-\hat{\theta}(C_n,t)\big)^2dt$, at sensors $C_{n=1,\ldots,N_c}$	[30–33, 37–39]
Eq.5	**Adjoint problem**	$\begin{cases}\rho C\frac{\partial\psi(x,y,t)}{\partial t}+\lambda\Delta\psi(x,y,t)=\mathrm{E}(x,y,t)+\frac{2h\psi(x,y,t)}{e} & \text{on } \Omega\times T\\ \psi(x,y,t_f)=0 & \text{on } \Omega\\ -\lambda\frac{\partial\psi(x,y,t)}{\partial\vec{n}}=0 & \text{on } \Gamma\times T\end{cases}$	[30–33, 37–39]
Eq.6	**Descent direction**	$d^{k+1}=-\nabla J(\theta;\Phi^k)+\frac{\left\|\nabla J(\theta;\Phi^k)\right\|^2}{\left\|\nabla J(\theta;\Phi^{k-1})\right\|^2}d^k$	[30–33, 37–39]
Eq.7	**Sensitivity problem**	$\begin{cases}\rho C\frac{\partial\delta\theta(x,y,t)}{\partial t}-\lambda\Delta\delta\theta(x,y,t)=\frac{\delta\Phi(x,y,t)-2h\delta\theta(x,y,t)}{e} & \text{on } \Omega\times T\\ \delta\theta(x,y,0)=0 & \text{on } \Omega\\ -\lambda\frac{\partial\delta\theta(x,y,t)}{\partial\vec{n}}=0 & \text{on } \Gamma\times T\end{cases}$	[30–33, 37–39]
Eq.8	**Descent depth**	$\gamma^{k+1}=\frac{\int_T\sum_{n=1}^{N_c}\Big(\theta(C_n,t;\Phi^k)-\hat{\theta}(C_n,t)\Big)\delta\theta(C_n,t;\Phi^k)dt}{\int_T\sum_{n=1}^{N_c}\delta\theta(C_n,t;\Phi^k)^2dt}$	[30–33, 37–39]
Eq.9	**Flux update**	$\phi^{k+1}=\phi^k-\gamma^{k+1}d^{k+1}$	[30–33, 37–39]

The heat transfer equation for the 3D aluminum plate is modeled by the following PDE:

$$\begin{cases} \rho C \dfrac{\partial \theta}{\partial t} - \lambda \Delta \theta = 0 & \text{in } \Omega \times T \\ \theta(x, y, z, 0) = \theta_0(x, y, z) & \text{in } \Omega \\ -\lambda \dfrac{\partial \theta}{\partial \vec{n}} = h(\theta - \theta_0) - \Phi & \text{on } \Gamma \times T \end{cases}$$

where Δ is the Laplace operator defined in Eq.2, and $\vec{n}$ is the boundary unit external normal vector. Thermophysical parameters $\{\rho, C, \lambda, h, \theta_0\}$ are given in Table 2, and are assumed constant. In fact, if the material used is heterogeneous, numerical resolution becomes more complex. The convective heat transfer coefficient h is in general difficult to determine as it highly depends on the particular environment surrounding the heat conductor (related to Navier-Stokes equations). However, this will be addressed in other articles.

To numerically evaluate the reliability of the proposed system for the unknown heat flux identification, fixed number of sensors aiming to collect temperature data during the experiment are positioned on Ω surface. However, the measurements are affected by Gaussian noises $\mathcal{N}(0, 1)$, thus rendering errors in the data collection process. Due to the plate negligible thickness, this study will focus on a 2D geometry defined now as:

$$(x, y) \in \Omega = \left]-\frac{L}{2}, +\frac{L}{2}\right[\times \left]-\frac{L}{2}, +\frac{L}{2}\right[\subset \mathbb{R}^2$$

with $\Gamma = \partial\Omega \subset \mathbb{R}$, and the corresponding PDE in Eq.3. Thus, Eq.1 and Eq.2 are regarded without the inclusion of the variable z.

2.3 Inverse problem

The heat flux density $\phi(t)$ is unknown, and is estimated by implementing the Conjugate Gradient Method (CGM), [37, 40]. In fact, the aluminum plate is experimentally heated by a heat source, and the Optris infrared camera performs acquisition by capturing images and converting them into pointwise temperature measurements $\hat{\theta}(x, y, t)$, which are then compared with the temperature simulated on COMSOL Multiphysics connected to MATLAB to calculate the cost function in Eq.4. Then, the CGM algorithm is iterated to identify $\phi(t)$, which is added into the mathematical model simulated again to compare the resulting temperature with the measured data until the cost function reaches the desired value J_{stop}, and thus the identification process stops (see Fig.2).

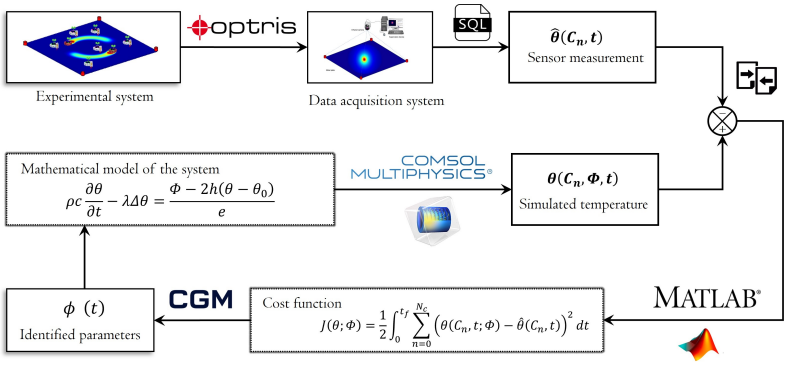

Fig. 2. Presentation of the CGM inverse problem.

A thermal engineering application is presented in [11] and its regularization properties are studied in [13]. The CGM is based on three well posed problems:

- Direct problem (Eq.3) for calculating temperature $\theta(x, y, t)$ corresponding to the estimated flux $\phi(t)$ at iteration k, then deducing criterion $J(\theta, \phi)$ (Eq.4) using measured temperature $\hat{\theta}(x, y, t)$.
- Adjoint problem (Eq.5) (written in terms of the Lagrangian $\psi(x, y, t)$ and $E(x, y, t)$ defined in [30–33, 37–39]) for deducing the cost function gradient and the descent direction (Eq.6).
- Sensitivity problem (Eq.7) for calculating the sensitivity function $\delta\theta(x, y, t)$ defined as the variation of temperature induced by variation of the heat flux in the descent direction, and then deducing the descent depth (Eq.8).

After solving these problems, the flux value $\phi(t)$ is updated (Eq.9).

3 Prototype validation results and discussions

3.1 Data acquisition results

Methods for temperature acquisition have been widely discussed in papers including analog temperature sensors connected to Arduino boards [1, 4], temperature measurement via snapshot hyper-spectral imaging systems [2], distributed fiber optic sensors [20], contact pyrometers [3, 5], and non-contact pyrometers [39].

In this study, an experiment was applied on an aluminum plate heated by a fixed centered heat source. The Optris PI 640i camera measured continuously the temperature on the plate surface by capturing heat propagation and providing a high-resolution thermal map. The collected data was visualized through coded images, with each pixel color corresponding to the temperature at a specific point on the plate. These infrared images were converted to matrices in MATLAB, each matrix element representing a pixel's temperature data (see Fig.3). Figure 4a shows the aluminum plate temperature at a recorded data instant corresponding

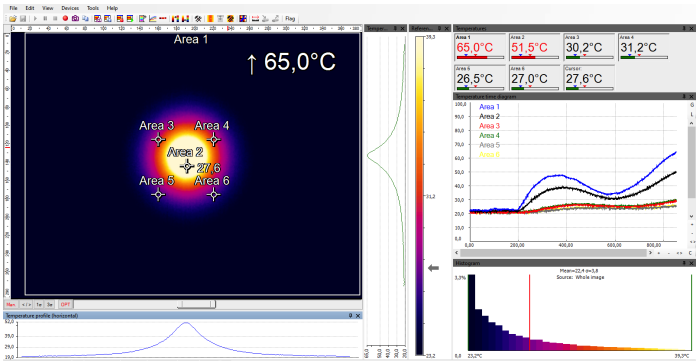

Fig. 3. Presentation of Optris software for the connecting infrared camera.

to 10 minutes of heating. Additionally, Fig.5a provides a time-series plot of the temperature at the plate center and progressively farther points. This indicates how the central area reaches a higher temperature faster than the peripheral regions.

After detailing the data acquisition methodology using the Optris PI 640i infrared camera to capture real-time temperature distributions, the focus now shifts to the modeling phase of the study. In fact, the precise experimental data served as a foundational benchmark for validating the subsequent theoretical frameworks.

3.2 Direct problem simulation results

The constructed model replicates the experimental setup, where a fixed heat source is centrally placed on an aluminum plate, and relevant parameters such as $\{\rho C, \lambda, h, \theta_0, t_f\}$ are defined based on the experimental prototype conditions (see Table 2). Thus direct problem in Eq.3 for predicting temperature distribution over time is numerically simulated by the Finite element method (FEM) implemented with COMSOL Multiphysics and MATLAB. Therefore, the results after 10 minutes of central heating are shown in Fig.4b.

Table 2. Mathematical model input parameters

Symbol	Definition	Value
ρC	Volumetric heat capacity	$2.421.10^6$ J $\cdot$ m^{-3} $\cdot$ K^{-1}
h	Natural convection	10 W $\cdot$ m^{-2} $\cdot$ K^{-1}
λ	Thermal conductivity	237 W $\cdot$ m^{-1} $\cdot$ K^{-1}
θ_0	Initial temperature	21 °C
t_f	Final time	600 s

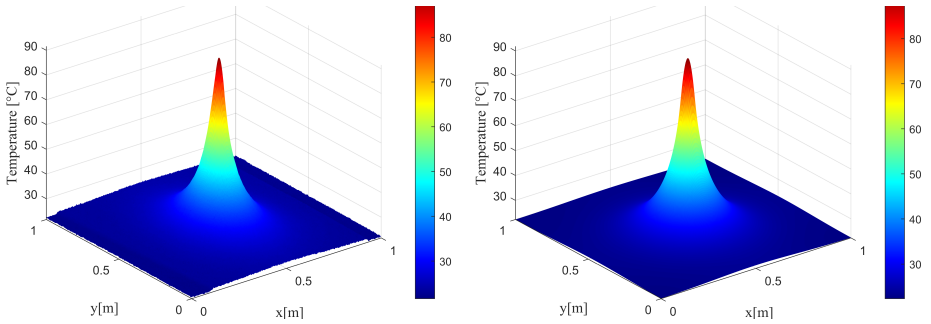

(a) Real temperature distribution. (b) Simulated temperature distribution.

Fig. 4. Temperature distribution at final time.

Model structure validation is crucial in ensuring the accuracy of the simulation and the proposed system parameter identification methods. Figures 4a and 4b illustrating respectively temperature distribution during the experiment and direct problem simulation, are similar. However, it is necessary to perform various tests to ensure the theoretical model precision.

3.3 Theoretical modeling validation results

The simulated temperature evolution over time at specific points on the aluminum plate is compared with real measurements in Fig.5b, corresponding to the sensor located at the center of the plate.

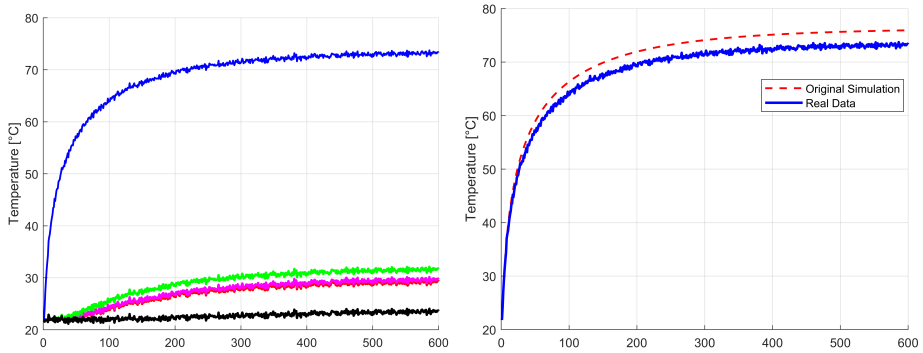

(a) Real sensors variation. (b) Real and simulated data comparison.

Fig. 5. Temperature sensors variation for model validation.

This proves that the proposed prototype can satisfy the theoretical model. However, it is necessary to calculate the multi-sensors temperature residuals to determine the errors between simulated and measured temperatures (Fig.6).

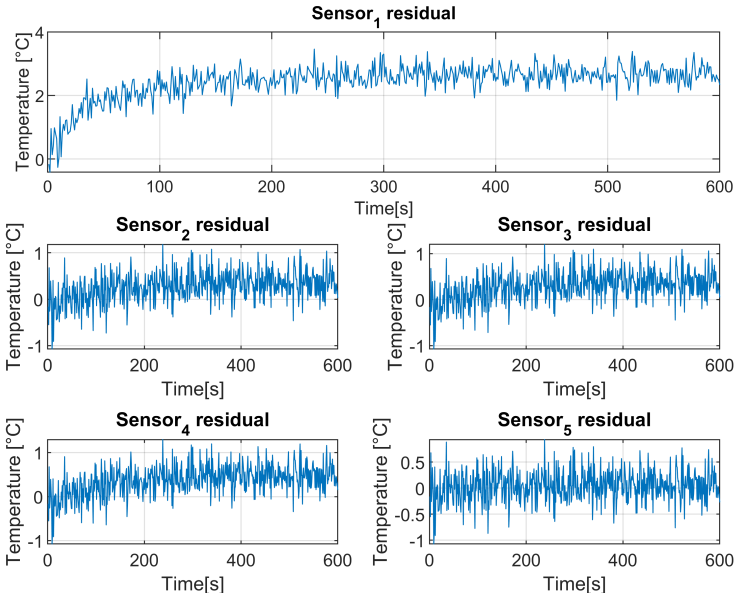

Fig. 6. Multi-sensor temperature residuals overview.

Even if the structure model (direct problem in Eq.3) is validated, an accurate identification has to be investigated in order to determine the heat spatial domain, the heat flux versus time, and the delay. Accordingly, several system parameter identification campaigns will be proposed including offline mode, quasi-online mode, quasi-online mode with prediction. Elaborate studies will be discussed, and their results will be published in the next articles.

4 Conclusions and perspectives

The successful validation of the direct problem model using COMSOL Multiphysics and MATLAB has provided a solid foundation for advancing to more complex thermal analyses, notably the inverse heat conduction problem (IHCP). The latter poses unique challenges, primarily due to its ill-posed nature. In fact, by leveraging the accuracy of our validated direct problem model, stability and reliability of inverse problems could be enhanced.

In the forthcoming work, the aim is to control and implement regularization techniques for identifying temporal variation of the unknown heat flux applied to the aluminum plate, thus ensuring a robust convergence of the simulated

temperature to the measured data. This is critical in applications requiring precise control of thermal processes, and helps in smoothing out the IHCPs noises. Furthermore, comparative analysis of different regularization methods will be conducted to determine the optimal approach for this specific application. Ultimately, the progression from model validation to solving IHCPs not only enhances the understanding of thermal behaviors but also improves the capability to manipulate them in practical scenarios.

References

1. H. Gad and H. E. Gad, "Development of a new temperature data acquisition system for solar energy applications," *Renewable energy*, vol. 74, pp. 337–343, 2015.
2. A. Gorevoy, A. Machikhin, A. Bykov, and A. Kren, "Optimization of data acquisition algorithm for temperature and emissivity distribution measurement using snapshot hyperspectral imaging systems," *Case Studies in Thermal Engineering*, vol. 26, p. 101154, 2021.
3. Y. Huang, Y. Pan, C. Li, M. Long, D. Chen, Z. Yang, and J. Long, "Real-time surface temperature measurement of steel continuous casting strand in the steam-filled spray chamber," *International Journal of Thermal Sciences*, vol. 199, p. 108909, 2024.
4. M. Kunicki, S. Borucki, D. Zmarzły, and J. Frymus, "Data acquisition system for on-line temperature monitoring in power transformers," *Measurement*, vol. 161, p. 107909, 2020.
5. G. Wang, Y. Bai, N. Yan, L. Li, K. Zhang, B. Zhao, Y. Liu, and K. Yu, "Investigation into x-point emissivity in metallic materials for temperature measurement," *Case Studies in Thermal Engineering*, p. 104371, 2024.
6. G. Bao, J.-M. Coron, and T. Li, *Control and Inverse Problems for Partial Differential Equations*. World Scientific, 2019, vol. 22.
7. E. Hensel, *Inverse theory and applications for engineers*. Prentice Hall Englewood Cliffs, NJ, 1991, vol. 199, no. 1.
8. C. Le Niliot and F. Lefèvre, "A parameter estimation approach to solve the inverse problem of point heat sources identification," *International Journal of Heat and Mass Transfer*, vol. 47, no. 4, pp. 827–841, 2004.
9. H. R. Orlande, *Inverse heat transfer: fundamentals and applications*. CRC Press, 2021.
10. O. M. Alifanov, *Iterative Regularization of Inverse Problems*. Berlin, Heidelberg: Springer Berlin Heidelberg, 1994, pp. 227–328.
11. Y. Jarny, M. Ozisik, and J. Bardon, "A general optimization method using adjoint equation for solving multidimensional inverse heat conduction," *International journal of heat and mass transfer*, vol. 34, no. 11, pp. 2911–2919, 1991.
12. L. Perez, L. Autrique, and M. Gillet, "Implementation of a conjugate gradient algorithm for thermal diffusivity identification in a moving boundaries system," in *Journal of Physics: Conference Series*, vol. 135, no. 1. IOP Publishing, 2008, p. 012082.
13. M. Prud'homme and T. H. Nguyen, "On the iterative regularization of inverse heat conduction problems by conjugate gradient method," *International Communications in Heat and Mass Transfer*, vol. 25, no. 7, pp. 999–1008, 1998.

14. T. Azar, "Développement de stratégies de commandes pour des systèmes décrits par des équations aux dérivées partielles paraboliques non linéaires," Ph.D. dissertation, Université d'Angers, 2021.
15. T. Azar, L. Perez, C. Prieur, E. Moulay, and L. Autrique, "Quasi-online disturbance rejection for nonlinear parabolic pde using a receding time horizon control," in *2021 European Control Conference (ECC)*. IEEE, 2021, pp. 2603–2610.
16. T. Azar, L. Perez, C. Prieur, E. Moulay, and L.Autrique, "Stabilization using in-domain actuator: a numerical method for a non linear parabolic partial differential equation," in *CONTROLO 2020: Proceedings of the 14th APCA International Conference on Automatic Control and Soft Computing, July 1-3, 2020, Bragança, Portugal*. Springer, 2021, pp. 616–627.
17. A. S. Neto and M. Özişik, "Simultaneous estimation of location and timewise-varying strength of a plane heat source," *Numerical Heat Transfer, Part A: Applications*, vol. 24, no. 4, pp. 467–477, 1993.
18. A. Hasanov, "Identification of spacewise and time dependent source terms in 1d heat conduction equation from temperature measurement at a final time," *International Journal of Heat and Mass Transfer*, vol. 55, no. 7-8, pp. 2069–2080, 2012.
19. Z. Yi and D. Murio, "Source term identification in 1-d ihcp," *Computers & Mathematics with Applications*, vol. 47, no. 12, pp. 1921–1933, 2004.
20. Y. Zhu and G. Chen, "Rayleigh scattering based, thermal-induced displacement measurement along a steel plate at high temperature," *Journal of Infrastructure Intelligence and Resilience*, vol. 1, no. 1, p. 100002, 2022.
21. M. S. Bidou, L. Perez, S. Verron, and L. Autrique, "Identification of failure times for a system governed by a non-linear parabolic partial differential equation," *IFAC-PapersOnLine*, vol. 55, no. 40, pp. 37–42, 2022.
22. M. S. Bidou, S. Verron, L. Perez, and L. Autrique, "Kalman smoother for detection of heat sources defects," in *2022 international conference on control, automation and diagnosis (ICCAD)*. IEEE, 2022, pp. 1–6.
23. M.-S. Bidou, S. Verron, L. Perez, and L. Autrique, "Bayesian filter for failure times identification of moving heat sources in 2d geometry," *International Journal of Systems Science*, vol. 55, no. 4, pp. 671–686, 2024.
24. M. S. Bidou, L. Perez, S. Verron, and L. Autrique, "A model-based failure times identification for a system governed by a 2d parabolic partial differential equation," *IET Control Theory & Applications*, 2024.
25. S. Fakih, L. Perez, and L. Autrique, "Stabilization in finite time for a thermal system described by a parabolic partial differential equation in a 2d geometry," in *10th International Conference on Control, Decision and Information Technologies*, 2024.
26. C. Le Niliot and F. Lefèvre, "A method for multiple steady line heat sources identification in a diffusive system: application to an experimental 2d problem," *International Journal of Heat and Mass Transfer*, vol. 44, no. 7, pp. 1425–1438, 2001.
27. L. Ling, M. Yamamoto, Y. Hon, and T. Takeuchi, "Identification of source locations in two-dimensional heat equations," *Inverse Problems*, vol. 22, no. 4, p. 1289, 2006.
28. L. Ling and T. Takeuchi, "Point sources identification problems for heat equations," *Commun. Comput. Phys*, vol. 5, no. 5, pp. 897–913, 2009.
29. M. S. Bidou, L. Perez, S. Verron, and L. Autrique, "Quasi-online failure times identification of mobile heat sources in 2d geometry," *Journal of Process Control*, vol. 136, p. 103183, 2024.
30. T. P. Tran, "Control strategies of mobiles sensors for quasi on-line identification of mobile heating source," PhD Thesis, University of Angers, Jun. 2017.

31. A. Vergnaud, G. Beaugrand, O. Gaye, L. Perez, P. Lucidarme, and L. Autrique, "On-line identification of temperature-dependent thermal conductivity," in *2014 European Control Conference (ECC)*. IEEE, 2014, pp. 2139–2144.
32. A. Vergnaud, L. Perez, and L. Autrique, "Quasi-online parametric identification of moving heating devices in a 2d geometry," *International Journal of Thermal Sciences*, vol. 102, pp. 47–61, 2016.
33. A.Vergnaud, L. Perez, and L. Autrique, "Adaptive selection of relevant sensors in a network for unknown mobile heating flux estimation," *IEEE Sensors Journal*, vol. 20, pp. 15 133–15 142, 2020.
34. L. Autrique, N. Ramdani, and S. Rodier, "Mobile source estimation with an iterative regularization method," in *5th International Conference on Inverse Problems in Engineering: Theory and Practice, Cambridge, UK*, vol. 11, no. 15, 2005.
35. S. Beddiaf, L. Perez, L. Autrique, and J.-C. Jolly, "Simultaneous determination of time-varying strength and location of a heating source in a three-dimensional domain," *Inverse problems in science and engineering*, vol. 22, no. 1, pp. 166–183, 2014.
36. S. Beddiaf, L. Autrique, L. Perez, and J.-C. Jolly, "Time-dependent heat flux identification: Application to a three-dimensional inverse heat conduction problem," in *2012 Proceedings of International Conference on Modelling, Identification and Control*. IEEE, 2012, pp. 1242–1248.
37. A. Vergnaud, T. P. Tran, L. Perez, P. Lucidarme, and L. Autrique, "Deployment strategies of mobile sensors for monitoring of mobile sources: method and prototype," in *Control Architectures of Robots 2015, 10th National Conference*, Lyon, France, Jun. 2015.
38. Tran, Thanh-Phong, "Unknown parameter identification of mobile heating source by using the sensitivity of sensor network," *ITM Web Conf.*, vol. 20, p. 02013, 2018.
39. T. P. Tran, L. Perez, and L. Autrique, "Quasi-online method for the identification of heat flux densities and trajectories of two mobile heating sources," in *2017 11th Asian Control Conference (ASCC)*. IEEE, 2017, pp. 1395–1400.
40. J. F. Bonnans, J. C. Gilbert, C. Lemaréchal, and C. A. Sagastizábal, *Mathematical Programming: Theory and Algorithms*. Springer-Verlag, 1983, vol. 1.